Brain Topography (2025) 38:47
https://doi.org/10.1007/s10548-025-01119-w

ORIGINAL PAPER

Assessing Brain Network Dynamics During Postural Control Task Using EEG Microstates

Carmine Gelormini[1] · Lorena Guerrini[1,2] · Federica Pescaglia[1] · Romain Aubonnet[3] · Halldór Jónsson Jr[4] · Hannes Petersen[5,6] · Giorgio Di Lorenzo[3,7] · Paolo Gargiulo[1,8]

Received: 7 November 2024 / Accepted: 15 May 2025 / Published online: 3 June 2025

Abstract
The ability to maintain our body's balance and stability in space is crucial for performing daily activities. Effective postural control (PC) strategies rely on integrating visual, vestibular, and proprioceptive sensory inputs. While neuroimaging has revealed key areas involved in PC—including brainstem, cerebellum, and cortical networks—the rapid neural mechanisms underlying dynamic postural tasks remain less understood. Therefore, we used EEG microstate analysis within the BioVRSea experiment to explore the temporal brain dynamics that support PC. This complex paradigm simulates maintaining an upright posture on a moving platform, integrated with virtual reality (VR), to replicate the sensation of balancing on a boat. Data were acquired from 266 healthy subjects using a 64-channel EEG system. Using a modified k-means method, five EEG microstate maps were identified to best model the paradigm. Differences in each microstate maps feature (occurrence, duration, and coverage) between experimental phases were analyzed using a linear mixed model, revealing significant differences between microstates within the experiment phases. The temporal parameters of microstate C showed significantly higher levels in all experimental phases compared to other microstate maps, whereas microstate B displayed an opposite pattern, consistently showing lower levels. This study marks the first attempt to use microstate analysis during a dynamic task, demonstrating the decisive role of microstate C and, conversely, microstate B in differentiating the PC phases. These results demonstrate the utility of microstate technique in studying temporal brain dynamics during PC, with potential applications in the early detection of neurodegenerative diseases.

Keywords Electroencephalography (EEG) · Microstates · Neural Networks · Temporal Brain Dynamics · Postural Control · Virtual Reality

Introduction

Postural control (PC) refers to the ability to maintain the body's balance and stability in space by regulating the position of the center of gravity relative to the base of support (Horak and Macpherson 1996; Pollock et al. 2000). Disruptions in PC can be linked to various conditions, including neurological disorders, injuries, and sensory impairments (Paillard and Noé 2015), making an understanding of postural instability crucial for effective diagnosis and treatment.

Communicated by Christoph Michel.

✉ Carmine Gelormini
carmine23@ru.is

1 Institute of Biomedical and Neural Engineering, Reykjavik University, Reykjavik, Iceland

2 Department of Engineering, University of Campania Luigi, Aversa, Italy

3 Laboratory of Psychophysiology and Cognitive Neuroscience, Department of System Medicine, University of Rome Tor Vegata, Rome, Italy

4 Department of Orthopaedics, Landspitali University Hospital, Reykjavik, Iceland

5 Faculty of Medicine, University of Iceland, Reykjavik, Iceland

6 Akureyri Hospital, Akureyri, Iceland

7 IRCCS Fondazione Santa Lucia, Rome, Italy

8 Department of Science, Landspitali University Hospital, Reykjavik, Iceland

It is known that PC strategies rely on multisensory integration—combining vestibular, visual, and proprioceptive inputs—which help coordinate body posture relative to the external environment through predictive feedforward mechanisms (Fitzpatrick et al. 1996). An important aspect of PC takes place in the spinal cord, brainstem, and midbrain locomotor areas, while movement control involves supratentorial regions of the central nervous system (CNS) (Takakusaki 2017). Nonetheless, it remains unclear which regions of the CNS are involved in the regulation of disturbed PC tasks and, even more so, which parts are involved in adaptation to recurring disturbances. Recent studies have shed light on CNS areas involved in this process (Bonassi et al. 2024; Richer et al. 2024).

The vestibular system is critical for stabilizing gaze, controlling balance, and providing a subjective sense of motion and spatial orientation (Cullen 2012). Neuroimaging studies using functional magnetic resonance imaging (fMRI) have explored vestibular processing through techniques such as caloric (Fasold et al. 2002) and galvanic vestibular stimulation (Stephan et al. 2005). These studies have identified a network crucial for vestibular and multisensory processing, including regions such as the parieto-insular vestibular cortex (PIVC), superior temporal gyrus (STG), insular cortex, anterior cingulate gyrus, precuneus, and hippocampus (Dieterich and Brandt 2008; Herold et al. 2017). Furthermore, neurons that integrate visual and vestibular signals for self-motion perception have been found in the dorsal portion of the medial superior temporal area, ventral intraparietal area, posterior parietal cortex, and the superior temporal polysensory area (DeAngelis and Angelaki 2012). Nevertheless, the neural mechanisms of vestibulo-visual integration in cortical networks remain poorly understood (Keshavarzi et al. 2023).

Current approaches to studying the CNS role in PC increasingly rely on non-invasive methods, such as electroencephalography (EEG) and various neuroimaging techniques (Bath and Wang 2024). A recent review (Dijkstra et al. 2020) of neuroimaging studies—including whole-brain positron emission tomography (PET) and fMRI in the context of PC tasks—has confirmed the engagement of a distributed neural network, including the brainstem, cerebellum, thalamus, basal ganglia, and various cortical regions: prefrontal cortex (PFC), supplementary motor area (SMA), premotor cortex (PMC), and sensorimotor cortex (SMC).

While neuroimaging methods like fMRI have advanced our understanding of CNS involvement in PC, they face limitations in capturing rapid neural processes in dynamic tasks (Bath and Wang 2024). Here, EEG microstate analysis offers a complementary approach with millisecond precision, capturing transient patterns that represent synchronized large-scale brain network states (Michel and Koenig 2018). EEG microstates are defined as distinct, quasi-stable states of brain activity identified in multichannel resting-state EEG signals, characterized by stable topographies of electric potentials that persist for 60–120 ms before transitioning to another configuration (Koenig et al. 2002; Michel and Koenig 2018). These brief states can repeat multiple times within a second, allowing for the analysis of their temporal dynamics and correlations with cognitive processes. Although many potential maps can be generated from multichannel recordings, most of the EEG signal—typically over 70% of the total topographic variance—can be effectively represented by a discrete number of key topographies (Khanna et al. 2015). Using techniques like cluster analysis, key statistical parameters can be extracted, such as the duration a microstate class remains stable (i.e., duration), the frequency of occurrence for each microstate independent of its individual duration (i.e., occurrence), and the proportion of total time that each microstate class occupies (i.e., coverage) (Michel and Koenig 2018).

Microstate analysis has predominantly been used to study resting-state conditions, with growing applications in task-related contexts (Michel and Koenig 2018; Tarailis et al. 2024). However, few studies have applied this method to motor tasks or dynamic postural challenges (Dipietro et al. 2012; Minguillon et al. 2014; Ertl et al. 2020; Deolindo et al. 2021). To address this gap, we aim to apply EEG microstate analysis to a novel PC framework: the BioVRSea paradigm (Recenti et al. 2021). This experimental setup simulates being at sea on a small boat, integrating immersive virtual reality (VR) with a moving platform that incrementally increases in motion. EEG data are recorded throughout the task, which includes distinct experiment phases of increasing platform movement designed to assess dynamic PC strategies under different sensory and motor perturbations.

These strategies involve adjusting the sensory inputs used for balance control, a process known as sensory reweighting (Peterka 2002). In this process, the brain dynamically shifts the emphasis among vestibular, visual, and proprioceptive inputs to maintain optimal balance. Our paradigm includes distinct experimental phases where dynamic visual stimulation is applied without corresponding motor stimulus.

Related work on the BioVRSea framework has explored brain network states (BNSs) that occur during tasks by using advanced source-space EEG networks combined with clustering algorithms. This research shows that BNS distribution coherently describes the different phases of the experiment, with specific transitions between the visual, motor, salience, and default mode networks (Aubonnet et al. 2023). This paradigm has also shown promise in assessing early-stage Parkinson's disease (PD) through machine-learning models (Jacob et al. 2023).

Here, we aim to explore how brain network dynamics, as captured by microstate analysis, relate to the PC strategies required to maintain stability under complex postural challenges. This will allow us to infer functional significance by

querying empirical findings associated with spatially similar microstate maps from other studies.

Materials and methods

Participants

Out of the 281 individuals who participated, 15 were excluded due to poor EEG data quality, resulting in a final sample of 266 participants. The mean age of the participants was 33 years (± 14.55), with an age range from 19 to 73 years. Among these, 166 were female (mean age 31.72 ± 13.52), 115 were male (mean age 34.78 ± 15.87), and 2 participants did not specify their gender (mean age 31). All participants reported being healthy, with no clinical conditions or pathologies. They were provided with detailed written information about the study and gave their signed informed consent.

BioVRSea Paradigm

Participants were prepared for the virtual reality (VR) and physiological measurement components of the experiment. Preparation included fitting a 64-electrode wet EEG cap (sampling frequency: 4096 Hz, ANT Neuro, Hengelo, The Netherlands). The EEG amplifier (ANT Neuro, Hengelo, The Netherlands) was connected to the cap and secured in a backpack, which also contained a tablet for EEG signal acquisition.

After removing their shoes, participants donned the backpack and stepped onto the force platform, which consists of two force plates (Virtualis, Montpellier, France). They adopted a bipedal stance with feet positioned over the force plates, ensuring proper contact for postural sway measurements. Participants were instructed to remain still and avoid walking as the force plates continuously recorded their center of pressure shifts. VR goggles were then placed on the participants, and the experimental protocol was explained. Instructions were provided by the experimenter throughout the protocol, ensuring that participants were guided through each phase as it occurred (Fig. 1).

The experiment starts with a baseline period (BASE), during which participants stand still on a stationary platform for 2 min, observing a calm, non-sea visual environment, such as a mountain view (Fig. 2a). The participants are instructed to stand with their arms at their side, and their feet positioned on the force platform; they are free to move their head and "navigate" through the virtual environment.

Subsequently, to introduce the visual motion stimulus before adding physical motion, the PRE phase starts, where participants stand quietly for 40 s with their hands by their sides, observing a dynamic sea scene from a first-person perspective on a boat (Fig. 2a) During this experimental phase, the sea simulation is purely visual, with no motion from the platform. After these 40 s, participants are instructed to grasp the bar positioned in front of them.

The platform then begins moving in synchronization with the sea scene in the VR goggles, gradually increasing its motion from 25 to 75% of maximum wave amplitude. We refer to this motion sequence as the MOV phase, encompassing the 25%, 50%, and 75% platform wave amplitude phases, with each segment lasting 40 s. During this time, participants held onto the bars to maintain balance while observing the sea simulation.

Following the 75% phase, the POST phase starts. Platform motion is stopped, and participants are asked to release the bars and stand relaxed for a final 40 s while they see in

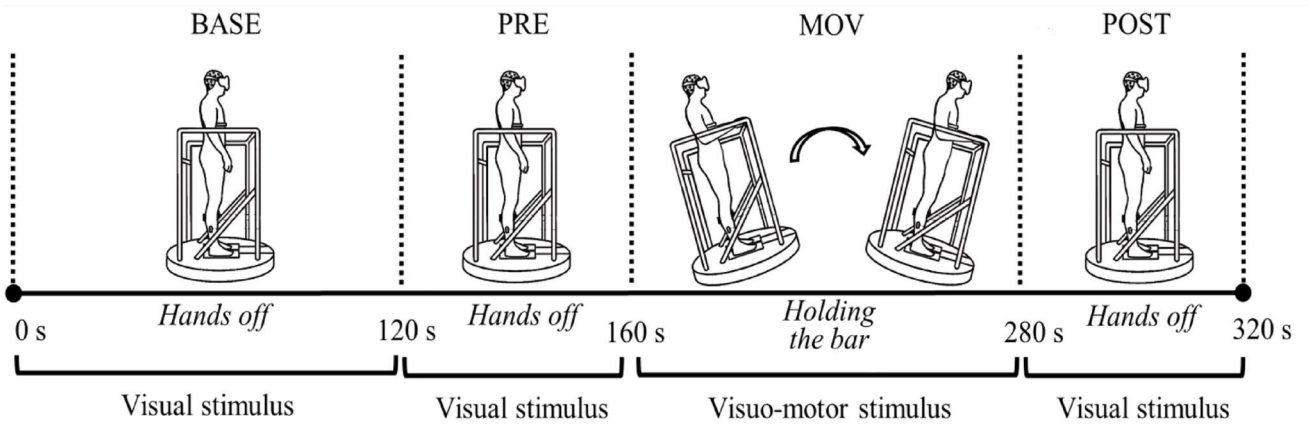

Fig. 1 The BioVRSea experimental protocol. In the BASE phase (0–120 s), participants stand still, observing a static scenario (mountain view) in VR, with hands off the bars. In the PRE phase (120–160 s), participants observe a dynamic sea scene in VR, still with their hands off the bars. In the MOV phase (160–280 s), participants hold the bars as the platform moves with increasing wave amplitudes (25%, 50%, 75%). The wave frequency can be set between 0.5 Hz and 3 Hz, and the wave amplitude between 0 and 2 mt. Finally, in the POST phase (280–320 s), participants release the bars and stand relaxed, observing the sea scene once again

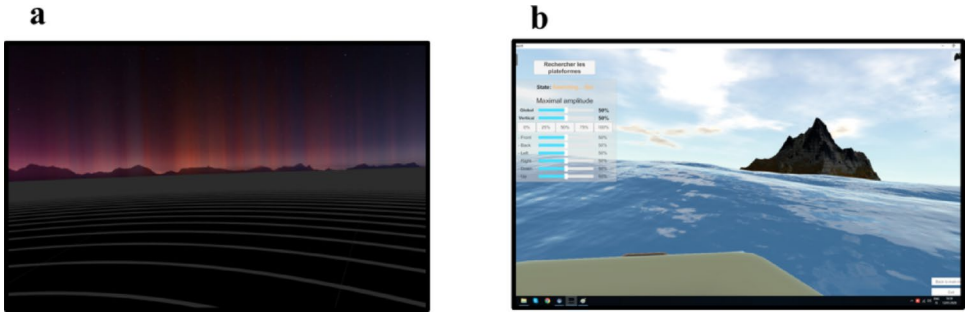

Fig. 2 **a** Mountain scenario during the BASE experimental phase **b** Dynamic Sea scene during the PRE, MOV, and POST experimental phases

the VR the dynamic sea scene of the PRE and MOV experimental phases. The POST phase replicates the conditions of the PRE phase. However, since participants had just experienced platform motion during the MOV phase, this phase might be perceived as more engaging due to the lingering effects of movement adaptation and the contrast between previous motion and current stillness.

For a more comprehensive description of the BioVRSea paradigm, see Jacob et al. (2022) and Recenti et al. (2022).

EEG Preprocessing

The EEGLAB Matlab Toolbox (Delorme and Makeig 2004) was used to pre-process and analyze the EEG data. To optimize computational resources while preserving critical signal integrity, the EEG data were downsampled to 512 Hz. The pre-processing protocol included applying a low-pass filter at 1 Hz and a high-pass filter at 45 Hz to enhance signal clarity and reduce noise.

Outlier channels were identified and removed based on kurtosis. The Automatic Subspace Reconstruction (ASR) algorithm was then applied to clean flat channels, channels with low correlation to neighbors, and those exhibiting excessive line noise. Additionally, line noise at 50 Hz and its harmonics were further reduced using the ZapLine algorithm (Klug and Kloosterman 2022). Channels with outlier spectral characteristics were also rejected.

Independent Component Analysis (ICA) using the Picard algorithm (Ablin et al. 2018) was conducted to separate neural from non-neural activity. The ICLabel tool (Pion-Tonachini et al. 2019) was employed to classify components, with non-brain components removed. ASR was reapplied to clean noisy signal bursts, using a burst criterion of 20. Finally, the data were re-referenced to the average of all channels.

EEG Microstate Analysis

Microstate analysis was performed using the MICROSTATELAB toolbox (Nagabhushan Kalburgi et al. 2024). Before extracting the microstate maps, a band-pass filter (2–20 Hz) was applied to isolate the relevant frequency bands. Next, individual microstate maps were identified using a modified K-means clustering algorithm (Pascual-Marqui et al. 1995), applied to the Global Field Power (GFP) peaks. The GFP at each time point was calculated as:

$$\mathrm{GFP}\,(t) = \sqrt{\frac{\sum_{1=1}^{N}\left(V_i\,(t) - \bar{V}\,(t)\right)^2}{N}},$$

where Vi(t) is the voltage at electrode i at time t, $\bar{V}$ (t) is the mean voltage across all electrodes at time t, and N is the number of electrodes (Khanna et al. 2015).

We explored four-to seven-cluster solutions, using a maximum of 100 restarts to ensure the stability and reliability of the identified clusters (see Figs. 5, 6, 7 and 8 in Appendix A). The GFP, which quantifies the variance of the potential field at each time point, was used to identify the most prominent time points for clustering (Milz et al. 2017). To determine the optimal number of microstate classes, the computed grand-mean maps were compared to established microstate topographies from previous literature by means of calculating the spatial correlation of each map with meta-microstate maps derived from studies using four to seven microstate solutions, employing the MS Template Explorer plugin (Koenig et al. 2024). Finally, we choose the solution with the highest average correlation, computed as the sum of the individual correlation values divided by the number of maps considered.

The sorted grand-mean microstate maps were fitted back to the original EEG data of each participant. Backfitting involves matching each time point in the EEG to the grand-mean microstate map, which shows the highest spatial correlation. This step assigns each time point to a specific microstate, allowing us to track which microstate is active at any given moment. Using this information, we calculated temporal parameters—such as duration, occurrence, and coverage—for each microstate class across the four phases of the experiment. The formulas for each temporal parameter are as follows:

1. Duration (/s): $\frac{T_i}{N_i}$;
2. Occurrence (/s): $\frac{N_i}{T_{total}}$;
3. Coverage (TC, %): $\frac{T_i}{T_{total}}$;

where T_i is the total time state$_i$ was active, N_i is the number of times state$_i$ was activated, and T_{total} is the total analysis time.

Statistical Analysis

The statistical analysis of the microstate temporal parameters was conducted using *R* version 4.3.1 (R Core Team 2021) with the *lme4* package (Bates et al. 2015). Given the longitudinal nature of the experiment and the hierarchical structure of the data, we fitted a linear mixed model (LMM) for each dependent variable (i.e., each microstate temporal parameter), estimated using Restricted Maximum Likelihood (REML). The model was formulated as follows:

$$MS\ temporal\ parameter \sim 1 + phase * microstate + (1|ID)$$

This formulation incorporated the interaction between different experimental phases (BASE, PRE, MOV, and POST) and microstate classes, with random effects for individual IDs.

An F-test was then performed to determine whether all fixed-effects coefficients were equal to zero, i.e., whether there was no significant relationship between the predictors (phase and microstate) and the outcome variables (microstate duration, occurrence, or coverage). Rejection of the null hypothesis indicated that at least one fixed-effects coefficient significantly differed from zero, suggesting that the corresponding predictor(s) significantly influenced the outcome variable.

Lastly, a post-hoc pairwise comparison between groups using the estimated marginal means was conducted with the *emmeans* package in R (Lenth 2024), applying the Bonferroni correction to adjust for multiple comparisons, with an alpha level set at 0.0083. This allowed us to identify specific significant differences in microstate duration, occurrence, and coverage across the various experimental phases and microstate classes.

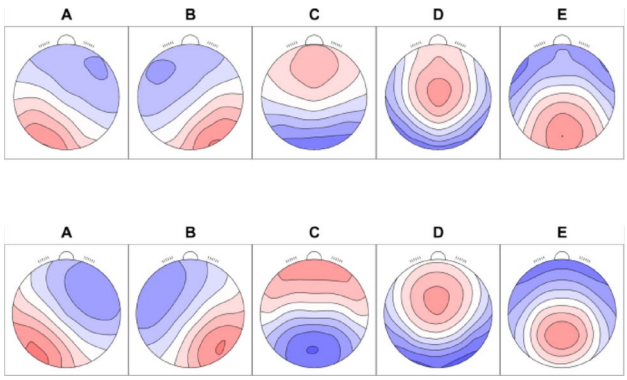

Fig. 3 **a** Computed Grand Mean microstate templates **b** Meta-microstates maps (Nagabhushan Kalburgi et al. 2024; Koenig et al. 2024)

Results

Number of Microstates

We selected five microstate maps (Fig. 3a) for analysis, specifically chosen based on their topographical similarities with the five-solution meta-microstate maps proposed by Nagabhushan Kalburgi et al. (2024). These meta-microstate maps represent spatial clusters of all microstate template maps across previously published studies (Koenig et al. 2024). The results of the similarity matrix (see Fig. 6b in Appendix A) indicated a notably high degree of shared variance between each of our selected microstate maps and their corresponding meta-microstate maps. Notably, Map B exhibited the highest similarity at 97.2%, suggesting a particularly strong correspondence with its meta-map. This was followed by Map E at 91.9%, Map D at 90.5%, Map A at 90.2%, and Map C at 80.9%.

Duration

The F-test from the Type III Analysis of Variance (ANOVA) (Table 1a) indicated that the factors of phase, microstate, and their interaction were statistically significant, with consistent results after adjusting for age and gender covariates. The results were as follows: *phase*: F (3, 5009.9) =4.1817, $p = 0.006$; *microstate*: F (4, 5012.0) =256.6119, $p < 0.001$; *phase* × *microstate* interaction: F (12, 5009.9) =3.132, $p < 0.001$. These findings suggest notable variations in microstate duration across different phases, revealing complex relationships unique to each microstate.

To further explore the significant interaction between phase and microstate, a post-hoc pairwise comparison of estimated marginal means was employed, and a Bonferroni correction was applied. The findings revealed that microstate C exhibited the longest average duration across all phases compared to other microstates. Microstate B demonstrated the shortest average duration during the PRE, MOV, and POST phases. Microstate A had the second-longest average duration during the BASE phase.

Notably, no significant differences between phases were observed for microstate C. However, a trend (mean diff. = 2.13590, $p = 0.0685$) was found for microstate B for the transition from the BASE to PRE phase, and significant

Table 1 ANOVA results from the *LMM* analysis for the *Duration*, *Occurrence*, and *Coverage* metrics

	Sum Sq	Mean Sq	NumDf	DenDF	F value	Pr(> F)
a ANOVA results from the LMM analysis for the variable Duration						
Phase	1186	395.4	3	5009.9	4.1817	0.0057695**
Microstate	97,065	24266.3	4	5012.0	256.6119	<0.001***
Phase: microstate	3555	296.2	12	5009.9	3.1324	<0.001***
b ANOVA results from the LMM analysis for the variable Occurrence						
Phase	2.09	0.698	3	5035	0.5025	0.580541
Microstate	686.49	171.622	4	5035	123.6440	<0.001***
Phase: microstate	40.12	3.343	12	5035	2.3940	0.004146**
c ANOVA results from the LMM analysis for the variable Coverage						
Phase	0	0.0	3	5300	0.0000	1.000
Microstate	66,997	16749.3	4	5300	194.0257	<0.001***
Phase: microstate	3147	262.2	12	5300	3.0375	<0.001***

Signif. codes: $p < 0.001$ '***'; $p < 0.01$ '**'; $p < 0.05$ '*'.

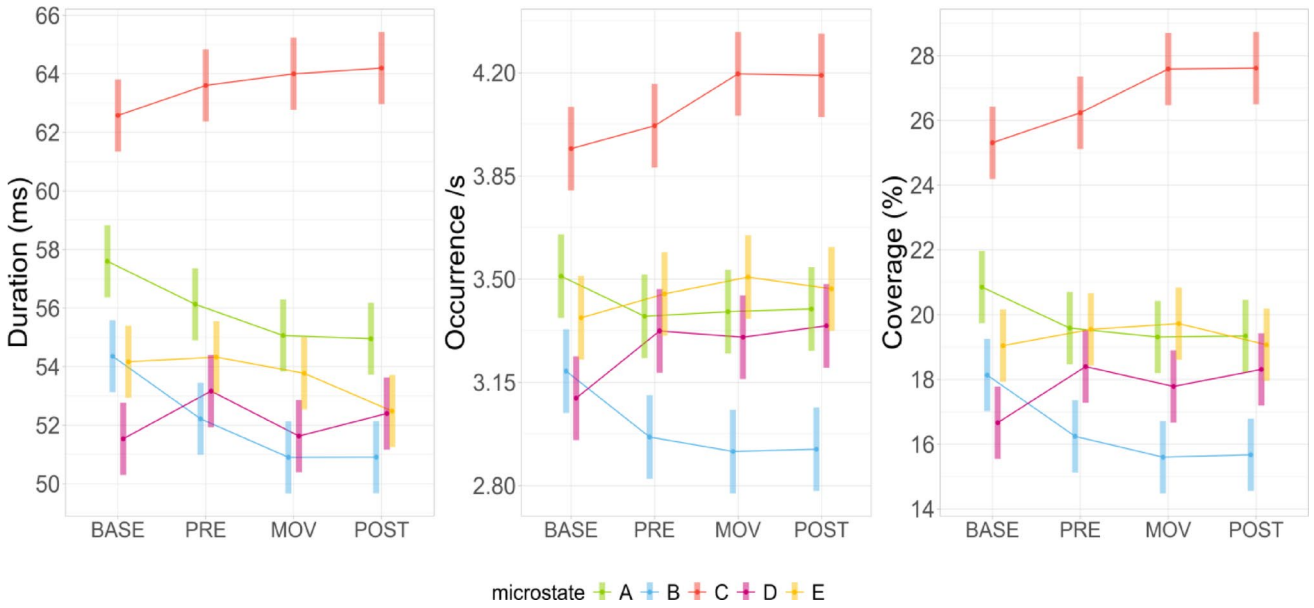

Fig. 4 Estimated marginal means along with their 95% confidence intervals for the three temporal parameters (Duration, Occurrence, and Coverage). *Duration*: Microstate C exhibits the longest duration, while microstate B significantly decreases over time: reductions are observed from BASE to MOV and from BASE to POST. *Occurrence*: Microstate C has the highest occurrence values. Conversely, microstate B decreases over time, with a significant reduction from BASE to MOV. Other microstate classes show relatively stable rates with minor fluctuations. *Coverage*: microstate C exhibits the highest coverage. Microstate C increases from BASE to MOV and from BASE to POST. In contrast, microstate B generally shows a decrease, with observed differences from BASE to MOV and from BASE to POST

differences from the BASE to both the MOV (mean diff. = −3.45107, $p = 0.0003$) and the POST (mean diff. = −3.44454, $p = 0.0003$) phases. For microstate A, significant differences were observed for the transition from BASE to MOV (mean diff. = −2.53568, $p = 0.0158$) and from BASE to POST phases (mean diff. = −2.64624, $p = 0.0102$). In contrast, the duration of microstates D and E did not vary significantly across experimental phases (see Fig. 4).

Occurrence

The F-test from the Type III ANOVA of the model (Table 1b) indicated that both the microstate class and its interaction with the phase had a significant influence on the occurrence metric, suggesting variability in how frequently each microstate appeared depending on the phase. These results were robust even with the inclusion of age and gender as covariates, confirming the stability of the observed effects: *phase*: F (3,5035) = 0.5025, $p = 0.5805$; *microstate*: F (4,5035) = 123.6440, $p < 0.001$; *phase* × *microstate* interaction: F (12,5035) = 2.3940, $p = 0.0041$.

Post-hoc pairwise comparisons revealed that microstate C was the most frequently occurring microstate across all phases. In contrast, microstate B consistently exhibited the lowest occurrence rate during the PRE, MOV, and POST phases. A statistically significant difference (mean diff. = 0.27259, $p =$

0.0457) was observed for microstate B between the BASE and MOV phases, but no significant differences were found for other microstates across experimental phases (see Fig. 4).

Coverage

The F-test from the Type III ANOVA of the model (Table 1c) showed significant effects regarding the coverage across different phases and microstates, independent of age and gender covariates. The results were as follows: *phase*: $F(3,5300) = 0.0000$, $p = 1.000$; *microstate*: $F(4,5300) = 194.0257$, $p < 0.001$; *phase* × *microstate* interaction: $F(12,5300) = 3.0375$, $p < 0.001$.

While the *phase* factor did not yield meaningful differences, indicating that the microstate classes were consistent in their dominance during the different experimental phases, the *microstate* factor significantly influenced coverage. Additionally, the interaction between *phase* and *microstate* was statistically significant, suggesting that the influence of microstate class on coverage varied depending on the phase.

Post-hoc pairwise comparisons revealed that microstate C exhibited the highest coverage, meaning it occupied the largest proportion of total recording time compared to the other microstate classes. Post-hoc pairwise comparisons highlighted significant phase-wise differences for microstate B and C. Specifically, microstate C demonstrated significant increases in coverage from BASE to MOV (mean diff. = 2.2772, $p = 0.0282$) and from BASE to POST (mean diff. = 2.3025, $p = 0.0256$), while microstate B showed a decrease from BASE to MOV (mean diff. = −2.5351, $p = 0.0099$) and from BASE to POST (mean diff. = −2.4626, $p = 0.0134$) (see Fig. 4).

Discussion

This study investigated the temporal dynamics of large-scale brain network activity involved in a complex postural control (PC) task using EEG microstate analysis. We explored how engagement in a dynamic and immersive virtual environment affects microstate patterns under varying levels of cognitive load and sensory input during the BioVRSea task (Recenti et al. 2021). By analyzing microstate dynamics, we aimed to observe how different brain network configurations support complex sensory integration in PC, potentially highlighting adaptations in neural processing associated with balance.

Previous research conducted during passive whole-body movements with weak accelerations observed that the EEG microstate architecture of four microstates remained invariant to weak whole-body accelerations (Ertl et al. 2020).

In contrast, our study, conducted in an immersive virtual environment, adopting five microstates, reveals distinct neural adaptations across experimental phases. Specifically, our findings demonstrate that microstates characterize postural PC tasks effectively, with microstate C playing a central role in balance maintenance. Furthermore, the robustness of our results is reinforced by the high number of participants, providing a strong foundation for understanding the neural dynamics of PC in complex sensory environments.

We analyzed microstate dynamics using a five-microstate configuration (Fig. 4a), finding strong topographical similarities when comparing our findings with published meta-microstate maps (Koenig et al. 2024). This supports the application of microstate technology in investigating complex, dynamic tasks.

During the BASE phase (quiet stance on a stable platform with a static visual scene), microstate C was significantly higher in duration, occurrence, and coverage than other maps.

In the PRE phase (dynamic visual stimulus simulating self-motion without platform movement), microstate B decreased, while microstate C remained stable and dominant. Microstate B exhibits a decreasing trend, though not statistically significant after Bonferroni correction.

Induced self-motion might result in vection, i.e., the subjective feeling of self-movement in a physically static observer, caused by a sensory mismatching between the visual and vestibular system (Reason and Brand 1975; Duffy 2000; Leung and Hon 2019), and ultimately can lead to motion sickness (Leung and Hon 2019; Reason and Brand 1975). Previous research (Bronstein 1995; Guerraz et al. 2001; Longridge et al. 2002) has shown that disruptions in the usual integration of visual and vestibular information are associated with a variety of conditions, with individuals affected by vestibular disorders exhibiting varying levels of cognitive impairment (Cronin et al. 2017; Li et al. 2024). Perceived self-motion might trigger sensory reweighting mechanisms, such as a reciprocal inhibitory visual-vestibular interaction (Brandt et al. 1998; Kleinschmidt 2002), that has been reported in different studies (Dieterich, 2007; Roberts et al. 2017).

In the MOV phase (platform oscillations synchronized with visual motion and participants holding a support bar), all microstates remained stable in all dynamics. This experimental phase is the most committing for the subject, as it involves the whole body and requires the active involvement of dynamic postural control mechanisms.

In the POST phase (active balance recovery after the mechanical perturbations without external support while exposed to visual perturbation), all microstate dynamics remained stable. Compensatory balance control, such as fixed-support PC strategies, may be initiated and mainly controlled via automatic postural responses (APRs) by means of subcortical-cortical loops. The relative stability of microstate dynamics in this phase might be attributed to the short latency of APRs, which may primarily involve

the spinal cord and midbrain rather than a transcortical loop (Jacobs and Horak 2007).

Overall, our findings highlight a marked difference between the static balance experimental phase and the dynamic balance phase, characterized by additional visual stimulation, during which the temporal dynamics of microstates A and B consistently decrease while the coverage of microstate C increases. The general dominance of microstate C across experimental phases suggests that his underlying brain network has a role in different PC strategies, while microstates B and A appear more sensitive to transitions between static and dynamic postural strategy. Instead, microstates D and E do not exhibit changes across the different experimental phases.

Literature on static PC tasks has reported widespread activation in the frontal, parietal, temporal, and occipital cortical areas and the cingulate cortex. During reactive postural control, subcortical (cerebellar and thalamic) and cortical activations have been observed, particularly in the supplementary motor area (SMA), premotor cortex, superior temporal gyrus, occipital cortex, and cingulate cortex. However, specific activation locations vary across studies. In contrast, dynamic postural control has been associated with brainstem, cerebellar, and thalamic activation, alongside engagement of the frontal lobe (including the SMA), parietal lobe, cingulate cortex, occipital lobe, and insula (for a comprehensive review, see Dijkstra et al., 2017).

The functional significance of microstates has been discussed across spontaneous, stimulus-induced, and pathological states (Koenig et al., 2002; Tarailis et al. 2024; Asha et al. 2024). Several studies have also associated EEG microstates with resting-state networks (RSNs) observed in fMRI (Britz et al., 2010; Musso et al., 2010; Pascual-Marqui et al. 2014; Custo et al. 2017). However, establishing direct correlations between EEG microstates and specific brain functions remains challenging (Michel and Koenig 2018). Pascual-Marqui and colleagues (2014) identified the cingulate cortex as a key region active in all four canonical microstates. Similarly, Custo and colleagues (2017) have found that seven resting-state microstates were linked to distinct neural activation patterns, with a shared brain network underlying all microstates. Common regions include areas along the anterior/posterior medial axes, the insula, and the superior parietal cortex.

Microstates A and B have been associated with sensory networks, auditory and visual (Milz et al. 2016; Michel and Koenig 2018). Microstate C has been associated with processing personally significant information, self-reflection, and self-referential mentation rather than purely autonomic processing; microstate D has been associated with attention processes and executive functioning and has underlying sources in the Dorsal Attention network; microstate E is related to interoceptive and emotional information processing, plays a role in certain cognitive functions, and is related to the salience network (Tarailis et al. 2024). Custo et al. (2017) indicated how microstate C and E are spatially correlated (correlation coefficient of 0.7).

Our experiment presents distinct visual and visuo-motor stimuli modulated at different time points to examine the brain's mechanisms of multisensory integration (Peterka 2002). Specifically, we expected meaningful differences in microstate temporal dynamics between experimental phases with congruent (BASE, MOV) and incongruent (PRE, MOV) stimulation, reflecting shifts in sensory reliance following postural perturbation (Peterka 2002; Mahboobin et al. 2005).

Although in our experiment microstate analysis does not allow us to observe sensory reweighting processes directly, it reveals a compelling pattern: during the experiment, microstate C features increased, while microstates A and B decreased. These findings align with previous research linking microstate dynamics to higher-order cognitive and emotional processes. Locomotor behaviors involve volitional, emotional, and automatic processes, with sensory information from multiple modalities modulating posture-gait control at different levels, including the brainstem, spinal cord, limbic system, and cerebral cortex (Jacobs and Horak 2007; Takakusaki 2023). Furthermore, accumulating evidence suggests that vestibular, emotional, and attentional networks overlap in key cortical and subcortical regions, reinforcing the idea that PC is shaped by the interplay of sensory, emotional, and cognitive mechanisms (Sibley et al. 2014; Barollo et al. 2022; Dieterich and Brandt 2024).

Krylova et al. (2021) found that microstate C was positively associated with vigilance, whereas microstates A and B exhibited the opposite pattern. Specifically, they observed a positive relationship between microstate C duration and vigilance, suggesting its role in cognitive control processes. Similarly, Hu et al. (2023) reported that increased occurrence and coverage of microstate C were associated with heightened emotional arousal. Further studies that have explored how microstates vary with emotional arousal and valence (Liu et al. 2023; Si et al. 2024) consistently found that high-arousal conditions lead to increased occurrence and coverage of microstate C.

Krylova et al. (2021) attributed the association between heightened vigilance and increased microstate C parameters to the hypothesis that enhanced temporal dynamics of microstate C reflect modulation of occipital alpha power. This hypothesis bridges the findings of Milz et al. (2017), who linked the appearance of specific microstates with the temporal and spatial distribution of the EEG alpha band, and of Olbrich et al. (2009), who observed that changes in vigilance stages were associated with alterations in occipital alpha activity. Altogether, this supports the role of alpha power in modulating brain states related to vigilance and cognitive processes and suggests that the modulation of alpha activity also plays a key role in the generation of EEG microstate classes.

We speculate that the dominance of microstate C in our study may not be exclusively related to multisensory integration but could also reflect changes in participants' emotional and arousal states. VR stimuli might further enhance emotional engagement and modulate arousal levels (Baumgartner et al. 2008; Weech et al. 2019).

Han and colleagues (2025) investigated the effect of VR-simulated scene intervention on cognitive fatigue recovery using four microstate maps. After VR intervention, they reported increased temporal parameters in class C and decreased parameters in classes B and D. Additionally, Hofmann and colleagues (2021) observed a relationship between arousal states in immersive VR experiences and cortical activity, finding that emotional arousal was associated with attenuation of alpha oscillatory activity in the parieto-occipital regions.

During emotionally arousing experiences, enhanced processing of relevant sensory stimuli serves as an adaptive response. The alpha frequency range contributes to functional inhibition of irrelevant sensory input (Kelly et al., 2006; Ma et al. 2022). Our previous research on the BioVRSea paradigm demonstrated alpha power modulation across all experimental phases compared to the baseline (Aubonnet et al. 2022), as well as phase-dependent changes in alpha power in response to visuomotor stimulation (Gelormini et al. 2024). Several studies investigating cortical dynamics during postural control tasks have identified alpha power modulation as a consistent feature in PC processes (Edwards et al. 2018; Peterson and Ferris 2018; Solis-Escalante et al. 2019).

The consistent dominance of microstate C, combined with previous findings of alpha power modulation in similar paradigms, hints at a possible functional relationship between these neural markers and arousal processes during balance tasks. However, while our findings suggest potential relationships between alpha oscillations, microstate C dynamics, and emotional processes during immersive experiences, these connections remain speculative.

Limitations

While our findings illustrate the efficacy of the microstate approach in modelling the neural strategies involved in the BioVRSea paradigm, several limitations warrant discussion.

The absence of a final baseline prevents assessing whether the observed effects are transient or lasting. Without a post-experiment measure, it remains unclear whether microstate dynamics return to their initial levels or persist over time. This limitation affects the interpretation of the findings, particularly in studies examining the brain's adaptive responses to sensory stimuli or VR interventions.

The microstate maps used in our analysis are primarily based on resting-state templates. While these templates align with our experimental context, their ability to accurately reflect task-specific microstates has not yet been demonstrated. Consequently, our interpretation of the results, although grounded in empirical knowledge of the BioVRSea paradigm, remains speculative regarding the functional significance of the observed microstates. Future studies should focus on defining and developing task-based microstates to improve the precision of EEG microstate analysis and validate them in dynamic environments.

Additionally, considering the dynamic nature of our paradigm, future research could benefit from examining transition probabilities and microstate sequences (Artoni et al. 2023). These analyses may reveal critical insights into the temporal dynamics of microstates and how the brain adapts its sensory integration strategies in response to environmental changes during PC tasks. By addressing these considerations, we can deepen our understanding of the neural mechanisms underlying balance and stability and improve the application of microstate analysis in related fields.

Conclusions

This study represents the first attempt, on a large dataset, employing EEG microstate analysis to display the brain network dynamics that characterize PC strategies during complex challenges. It emphasizes the effectiveness of EEG microstate analysis in revealing the dynamic brain configurations involved in PC during tasks within immersive virtual environments. The predominance of microstate C across experimental phases suggests its central role in PC, especially in maintaining balance during heightened sensory engagement. In contrast, the declining trends of microstates A and B reflect adaptive neural mechanisms in sensory processing. This research enhances our understanding of the neural adaptations involved in PC and provides valuable insights into the processes contributing to understanding balance disorders. Future studies should further investigate these microstate dynamics to clarify their significance in clinical contexts, especially in differentiating pathological cohorts like individuals with balance impairments related to neurodegenerative diseases—an area where the BioVRSea paradigm has already shown promise (Jacob et al. 2023).

Appendix A

See Figs. 5, 6, 7 and 8.

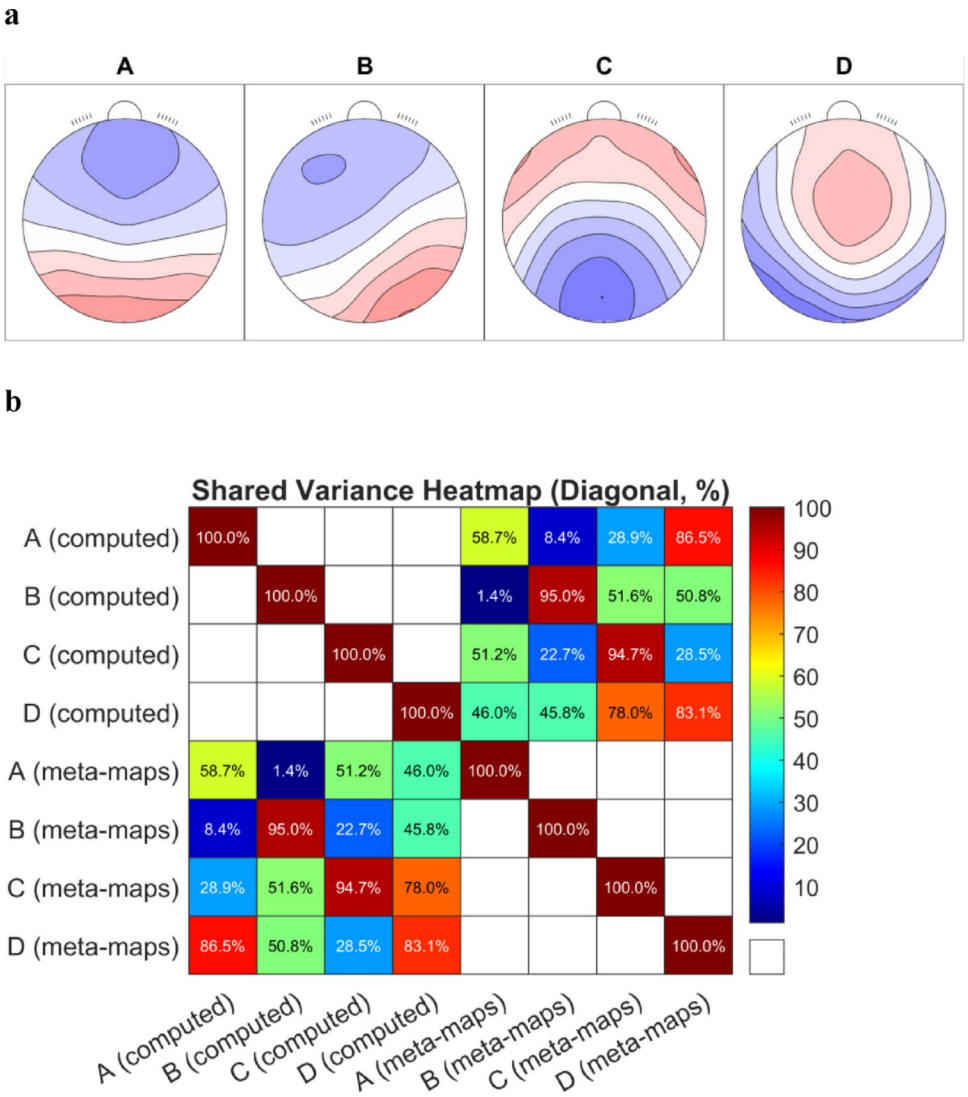

Fig. 5 Computed mean microstate templates b spatial correlation matrix with microstate meta-maps (4 solution template) (Koenig et al. 2024; Nagabhushan Kalburgi et al. 2024)

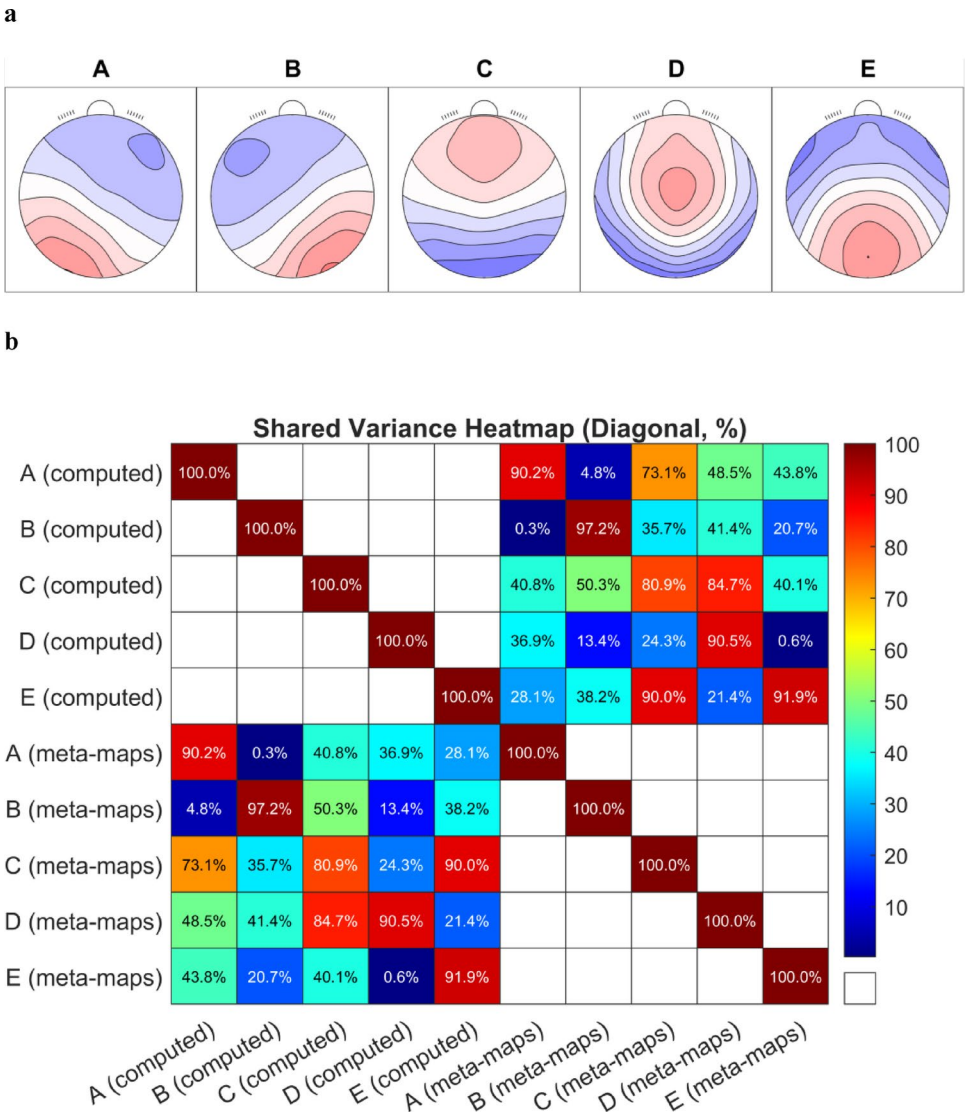

Fig. 6 a Computed mean microstate templates b spatial correlation matrix with microstate meta-maps (5 solution template) (Koenig et al. 2024; Nagabhushan Kalburgi et al. 2024)

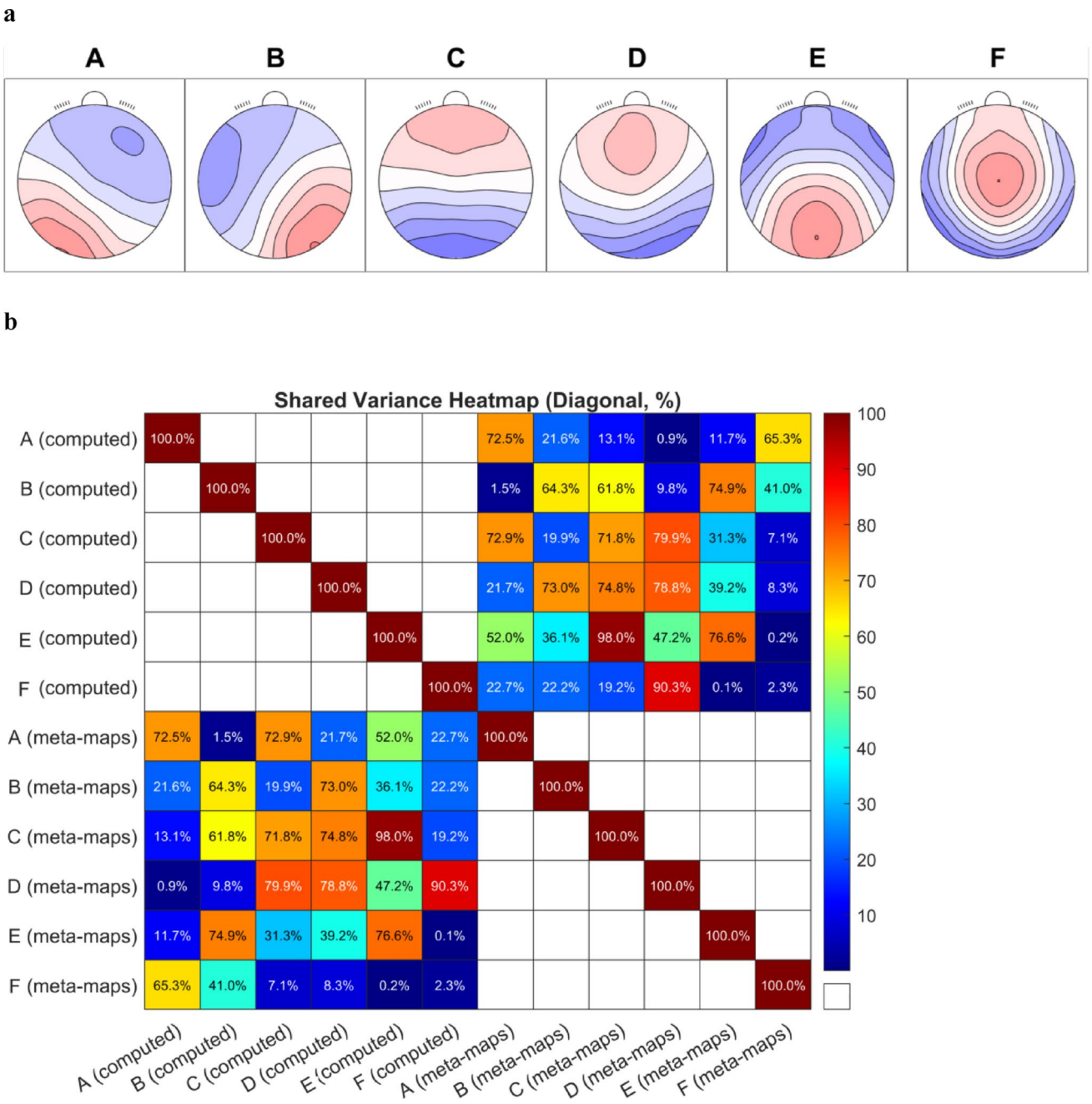

Fig. 7 a Computed mean microstate templates b spatial correlation matrix with microstate meta-maps (6 solutions template) (Koenig et al. 2024; Nagabhushan Kalburgi et al. 2024)

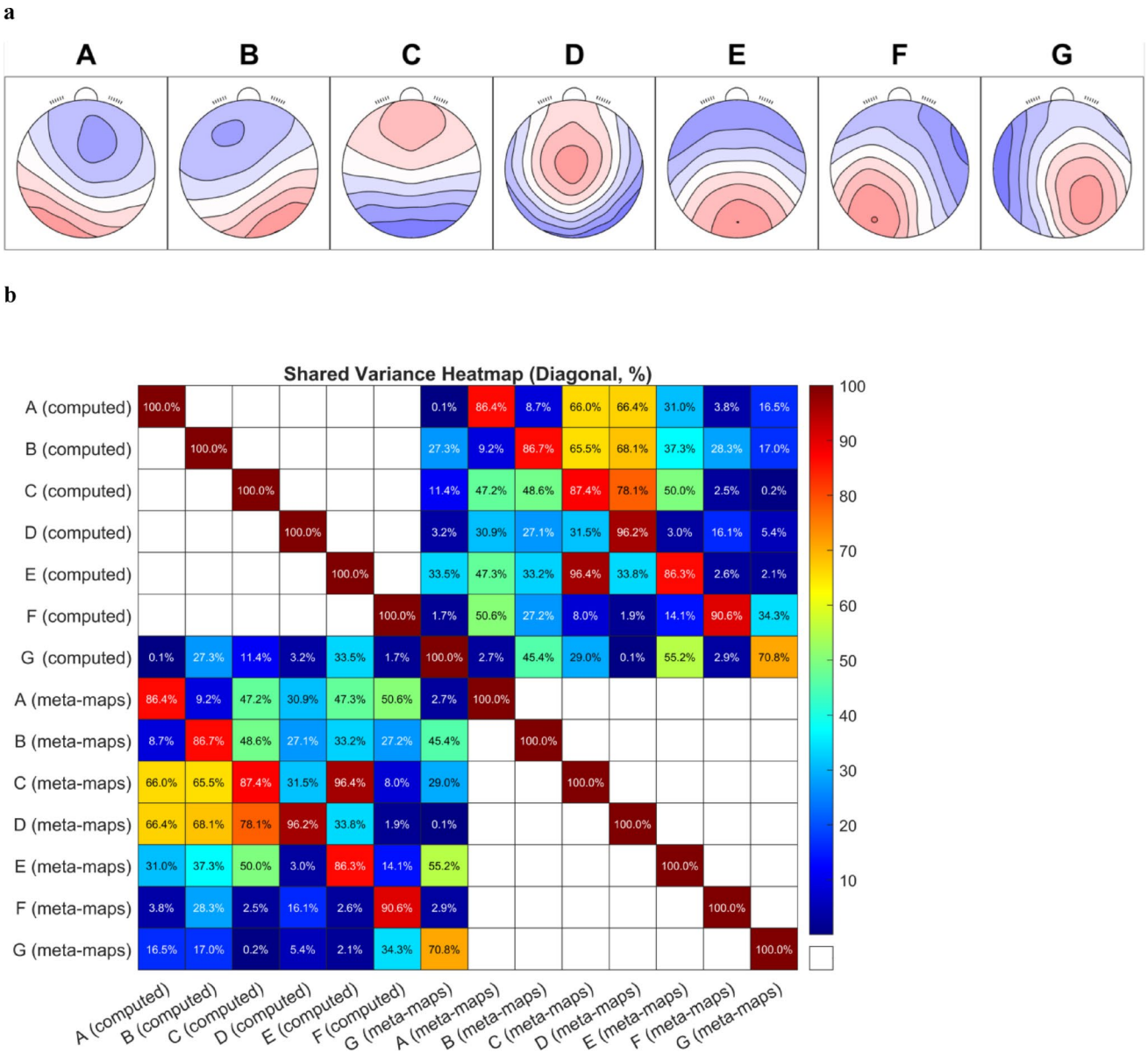

Fig. 8 a Computed mean microstate templates b spatial correlation matrix with microstate meta-maps (7 solutions template) (Koenig et al. 2024; Nagabhushan Kalburgi et al. 2024)

Acknowledgements This work was supported by RANNIS, the Icelandic Research Fund (Grant of Excellence no: 239612-051), and the Landspitali University Hospital research fund. GDL was supported by #NEXTGENERATIONEU (NGEU) and funded by the Ministry of University and Research (MUR), National Recovery and Resilience Plan (NRRP), project MNESYS (PE0000006)– (DN. 1553 11.10.2022).

Author Contributions Study concept and design: GDL, HP, and PG; Data collection: CG, LG, FP, HJ and RA; Analysis and interpretation of the data: CG, GDL, and PG; Software implementation: CG, GDL, and RA; writing—original draft: CG, GDL, and PG; writing—review and editing: HP, LG, FP, and RA.All authors reviewed the manuscript.

Data Availability No datasets were generated or analysed during the current study.

Declarations

Competing Interests The authors have no competing interests.

Ethics Approval The research was conducted in accordance with the principles outlined in the Declaration of Helsinki and adhered to Icelandic statutory requirements. The study protocol was approved by the Icelandic National Bioethics Committee (17-183-S1).

Informed Consent Informed consent was obtained from all individual participants included in the study.

References

Ablin P, Cardoso JF, Gramfort A (2018) Faster independent component analysis by preconditioning with Hessian approximations. IEEE Trans Signal Process 66(15):4040–4049. https://inria.hal.science/hal-01552340

Artoni F, Maillard J, Britz J, Brunet D, Lysakowski C, Tramèr MR, Michel CM (2023) Microsynt: exploring the syntax of EEG microstates. NeuroImage 277:120196. https://doi.org/10.1016/j.neuroimage.2023.120196

Asha SA, Sudalaimani C, Devanand P et al (2024) Analysis of EEG microstates as biomarkers in neuropsychological processes - Review. Comput Biol Med 173:108266. https://doi.org/10.1016/j.compbiomed.2024.108266

Aubonnet R, Shoykhet A, Jacob D, Di Lorenzo G, Petersen H, Gargiulo P (2022) Postural control paradigm (BioVRSea): towards a neurophysiological signature. Phys Meas 43(11). https://doi.org/10.1088/1361-6579/ac9c43

Aubonnet R, Hassan M, Mheich A, Di Lorenzo G, Petersen H, Gargiulo P (2023) Brain network dynamics in the alpha band during a complex postural control task. J Neural Eng 20(2). https://doi.org/10.1088/1741-2552/acc2e9

Barollo F, Hassan M, Petersen H, Rigoni I, Ramon C, Gargiulo P, Fratini A (2022) Cortical pathways during postural control: new insights from functional EEG source connectivity. IEEE Trans Neural Syst Rehabil Eng 30:72–84. https://doi.org/10.1109/TNSRE.2022.3140888

Bates D, Mächler M, Bolker B, Walker S (2015) Fitting linear mixed-effects models using lme4. J Stat Softw 67(1):1–48. https://doi.org/10.18637/jss.v067.i01

Bath JE, Wang DD (2024) Unraveling the threads of stability: a review of the neurophysiology of postural control in Parkinson's disease. Neurotherapeutics 21(3). https://doi.org/10.1016/j.neurot.2024.e00354

Baumgartner T, Speck D, Wettstein D, Masnari O, Beeli G, Jäncke L (2008) Feeling present in arousing virtual reality worlds: prefrontal brain regions differentially orchestrate presence experience in adults and children. Front Hum Neurosci 2:8. https://doi.org/10.3389/neuro.09.008.2008

Bonassi G, Zhao M, Samogin J et al (2024) Brain networks modulation during simple and complex gait: a mobile brain/body imaging study. Sensors 24(9):2875. https://doi.org/10.3390/s24092875

Brandt T, Bartenstein P, Janek A, Dieterich M (1998) Reciprocal inhibitory visual-vestibular interaction. Visual motion stimulation deactivates the parieto-insular vestibular cortex. Brain 121:1749–1758. https://doi.org/10.1093/brain/121.9.1749

Britz J, Van De Ville, Michel CM (2010) BOLD correlates of EEG topography reveal rapid resting-state network dynamics. NeuroImage 52(4):1162–1170. https://doi.org/10.1016/j.neuroimage.2010.02.052

Bronstein AM (1995) Visual vertigo syndrome: clinical and posturography findings. J Neurol Neurosurg Psychiatry 59(5):472–476. https://doi.org/10.1136/jnnp.59.5.472

R Core Team (2021) R: A language and environment for statistical computing. R Foundation for Statistical Computing, Vienna, Austria. URL https://www.R-project.org

Cronin T, Arshad Q, Seemungal BM (2017) Vestibular deficits in neurodegenerative disorders: balance, dizziness, and Spatial disorientation. Front Neurol 8:538. https://doi.org/10.3389/fneur.2017.00538

Cullen KE (2012) The vestibular system: multimodal integration and encoding of self-motion for motor control. Trends Neurosci 35(3):185–196. https://doi.org/10.1016/j.tins.2011.12.001

Custo A, Van De Ville D, Wells WM, Tomescu MI, Brunet D, Michel CM (2017) Electroencephalographic resting-state networks: source localization of microstates. Brain Connect 7(10):671–682. https://doi.org/10.1089/brain.2016.0476

DeAngelis GC, Angelaki DE (2012) Visual–vestibular integration for self-motion perception. In: Murray MM, Wallace MT (eds) The neural bases of multisensory processes. CRC Press/Taylor and Francis, Boca Raton, pp 629–652

Delorme A, Makeig S (2004) EEGLAB: an open source toolbox for analysis of single-trial EEG dynamics including independent component analysis. J Neurosci Methods 134(1):9–21. https://doi.org/10.1016/j.jneumeth.2003.10.009

Deolindo CS, Ribeiro MW, de Aratanha MAA, Scarpari JRS, Forster CHQ, da Silva RGA, Machado BS, Amaro Junior E, Koenig T, Kozasa EH (2021) Microstates in complex and dynamical environments: unraveling situational awareness in critical helicopter landing maneuvers. Hum Brain Mapp 42(10):3168–3181. https://doi.org/10.1002/hbm.25426

Dieterich M (2007) Functional brain imaging: a window into the visuo-vestibular systems. Curr Opin Neurol 20(1):12–18. https://doi.org/10.1097/WCO.0b013e328013f854

Dieterich M, Brandt T (2008) Functional brain imaging of peripheral and central vestibular disorders. Brain 131(10):2538–2552. https://doi.org/10.1093/brain/awn042

Dieterich M, Brandt T (2024) Central vestibular networking for sensorimotor control, cognition, and emotion. Curr Opin Neurol 37(1):74–82. https://journals.lww.com/co-neurology/fulltext/2024/02000/central_vestibular_networking_for_sensorimotor.11.aspx

Dijkstra BW, Bekkers EMJ, Gilat M, de Rond V, Hardwick RM, Nieuwboer A (2020) Functional neuroimaging of human postural control: A systematic review with meta-analysis. Neurosci Biobehav Rev 115:351–362. https://doi.org/10.1016/j.neubiorev.2020.04.028

Dipietro L, Plank M, Poizner H, Krebs H (2012) EEG microstate analysis in human motor corrections. In: Proc 4th IEEE/RAS-EMBS BioRob pp 1727–1732

Duffy CJ (2000) Optic flow analysis for self-movement perception. Int Rev Neurobiol 44:199–218

Edwards AE, Guven O, Furman MD, Arshad Q, Bronstein AM (2018) Electroencephalographic correlates of continuous postural tasks of increasing difficulty. Neurosci 395:35–48. https://doi.org/10.1016/j.neuroscience.2018.10.040

Ertl M, Schulte M, Dieterich M (2020) EEG microstate architecture does not change during passive whole-body accelerations. J Neurol 267:76–78. https://doi.org/10.1007/s00415-020-09794-4

Fasold O, von Brevern M, Kuhberg M, Ploner CJ, Villringer A, Lempert T, Wenzel R (2002) Human vestibular cortex as identified with caloric stimulation in functional magnetic resonance imaging. NeuroImage 17(3):1384–1393. https://doi.org/10.1006/nimg.2002.1241

Fitzpatrick R, Burke D, Gandevia SC (1996) Loop gain of reflexes controlling human standing measured with the use of postural and vestibular disturbances. J Neurophysiol 76(6):3994–4008. https://doi.org/10.1152/jn.1996.76.6.3994

Gelormini C, Guerrini L, Pescaglia F, Edmunds KJ, Aubonnet R, Recenti M, Di Lorenzo G, Gargiulo P (2024) Changes in EEG spectral power elicited during visual and motor stimuli with the BioVRSea paradigm. In: IEEE International Conference on Metrology for eXtended Reality, Artificial Intelligence and Neural Engineering (MetroXRAINE), St Albans, United Kingdom, 417–422. https://doi.org/10.1109/MetroXRAINE62247.2024.10796141

Guerraz M, Yardley L, Bertholon P, Pollak L, Rudge P, Gresty MA, Bronstein AM (2001) Visual vertigo: symptom assessment, Spatial orientation and postural control. Brain 124:1646–1656. https://doi.org/10.1093/brain/124.8.1646

Han JC, Jang KM, Choi Y et al (2025) Neuroimaging features for cognitive fatigue and its recovery with VR intervention: an EEG microstates analysis. Brain Res Bull 221:111223. https://doi.org/10.1016/j.brainresbull.2025.111223

Herold F, Orlowski K, Börmel S, Müller NG (2017) Cortical activation during balancing on a balance board. Hum Mov Sci 51:51–58. https://doi.org/10.1016/j.humov.2016.11.002

Hofmann SM, Weierich C, Poustka L et al (2021) Decoding subjective emotional arousal from EEG during an immersive virtual reality experience. eLife 10:e64812. https://doi.org/10.7554/eLife.64812

Horak FB, Macpherson JM (1996) Postural orientation and equilibrium. In: Shepard J, Rowell L (eds) Handbook of physiology. Exercise: regulation and integration of multiple systems. Oxford University Press, New York, pp 255–292

Hu W, Zhang Z, Zhao H, Zhang L, Li L, Huang G, Liang Z (2023) EEG microstate correlates of emotion dynamics and stimulation content during video watching. Cerebr Cort (New York N Y: 1991) 33(3):523–542. https://doi.org/10.1093/cercor/bhac082

Jacob D, Ingunn SU, Kristensen U, Aubonnet R et al (2022) Towards defining biomarkers to evaluate concussions using virtual reality and a moving platform (BioVRSea). Sci Rep 12(1):8996. https://doi.org/10.1038/s41598-022-12822-0

Jacob D, Guerrini L, Pescaglia F et al (2023) Adaptation strategies and neurophysiological response in early-stage Parkinson's disease: BioVRSea approach. Front Hum Neurosci 17:1197142. https://doi.org/10.3389/fnhum.2023.1197142

Jacobs JV, Horak F (2007) Cortical control of postural responses. J Neural Transm 114:1339–1348. https://doi.org/10.1007/s00702-007-0657-0

Kelly SP, Gomez-Ramirez M, Montague PR et al (2006) Increases in alpha oscillatory power reflect an active retinotopic mechanism for distracter suppression during sustained visuospatial attention. J Neurophysiol 95(6):3844–3851. https://doi.org/10.1152/jn.01234.2005

Keshavarzi S, Velez-Fort M, Margrie TW (2023) Cortical integration of vestibular and visual cues for navigation, visual processing, and perception. Annu Rev Neurosci 46:301–320. https://doi.org/10.1146/annurev-neuro-120722-100503

Khanna A, Pascual-Leone A, Michel CM, Farzan F (2015) Microstates in resting-state EEG: current status and future directions. Neurosci Biobehav Rev 49:105–113. https://doi.org/10.1016/j.neubiorev.2014.12.010

Kleinschmidt A (2002) Neural correlates of visual-motion perception as object- or self-motion. NeuroImage 16:873–882

Klug M, Kloosterman NA (2022) Zapline-plus: A zapline extension for automatic and adaptive removal of frequency-specific noise artifacts in M/EEG. Hum Brain Mapp 43:2743–2758. https://doi.org/10.1002/hbm.25832

Koenig T, Prichep LS, Lehmann D, Sosa PV, Braeker E, Kleinlogel H, Isenhart R, John ER (2002) Millisecond by millisecond, year by year: normative EEG microstates and developmental stages. NeuroImage 16(1):41–48. https://doi.org/10.1006/nimg.2002.1070

Koenig T, Diezig S, Kalburgi S et al (2024) EEG-Meta-Microstates: towards a more objective use of Resting-State EEG microstate findings across studies. Brain Topogr 37:218–231. https://doi.org/10.1007/s10548-023-00993-6

Krylova M, Alizadeh S, Izyurov I, Teckentrup V, Chang C, van der Meer J, Erb M, Kroemer N, Koenig T, Walter M, Jamalabadi H (2021) Evidence for modulation of EEG microstate sequence by vigilance level. NeuroImage 224:117393. https://doi.org/10.1016/j.neuroimage.2020.117393

Lenth R (2024) emmeans: Estimated Marginal Means, aka Least-Squares Means. R package version 1.10.5. https://rvlenth.github.io/emmeans/

Leung AK, Hon KL (2019) Motion sickness: an overview. Drugs Context 8:9–4. 10.7573

Li J, Xu X, Deng X, Li S, Guo T, Xie H (2024) Association of vestibular disorders and cognitive function: A systematic review. Laryngoscope. https://doi.org/10.1002/lary.31646

Liu J, Hu X, Shen X, Lv Z, Song S, Zhang D (2023) The EEG microstate representation of discrete emotions. Int J Psychophys 186:33–41. https://doi.org/10.1016/j.ijpsycho.2023.02.002

Longridge NS, Mallinson AI, Denton A (2002) Visual vestibular mismatch in patients treated with intratympanic gentamicin for Meniere's disease. J Otolaryngol 31(1):5–8. https://doi.org/10.2310/7070.2002.19125

Ma L, Marshall PJ, Wright WG (2022) The impact of external and internal focus of attention on visual dependence and EEG alpha oscillations during postural control. J Neur Eng Rehab 19(1):81. https://doi.org/10.1186/s12984-022-01059-7

Mahboobin A, Loughlin PJ, Redfern MS, Sparto J (2005) Sensory re-weighting in human postural control during moving-scene

perturbations. Exp Brain Res 167(2):260–267. https://doi.org/10.1007/s00221-005-0053-7
Michel CM, Koenig T (2018) EEG microstates as a tool for studying the Temporal dynamics of whole-brain neuronal networks: a review. NeuroImage 180:577–593. https://doi.org/10.1016/j.neuroimage.2017.11.062
Milz P, Michel CM, Koenig T (2016) The functional significance of EEG microstates—associations with modalities of thinking. NeuroImage 125:643–656. https://doi.org/10.1016/j.neuroimage.2015.08.023
Milz P, Pascual-Marqui RD, Achermann P, Kochi K, Faber PL (2017) The EEG microstate topography is predominantly determined by intracortical sources in the alpha band. NeuroImage 162:353–361. https://doi.org/10.1016/j.neuroimage.2017.08.058
Minguillon J, Pirondini E, Coscia M, Leeb R, Millan J, Van De Ville D, Micera S (2014) Modular organization of reaching and grasping movements investigated using EEG microstates. Annu Int Conf IEEE Eng Med Biol Soc 2093–2096. https://doi.org/10.1109/EMBC.2014.6944029
Musso F, Brinkmeyer J, Mobascher A et al (2010) Spontaneous brain activity and EEG microstates. A novel EEG/fMRI analysis approach to explore resting-state networks. Neuroimage 52(4):1149–1161. https://doi.org/10.1016/j.neuroimage.2010.01.093
Nagabhushan Kalburgi S, Kleinert T, Aryan D, Nash K, Schiller B, Koenig T (2024) MICROSTATELAB: the EEGLAB toolbox for Resting-State microstate analysis. Brain Topogr 37(4):621–645. https://doi.org/10.1007/s10548-023-01003-5
Olbrich S, Mulert C, Karch S, Trenner M, Leicht G, Pogarell O, Hegerl U (2009) EEG-vigilance and BOLD effect during simultaneous EEG/fMRI measurement. NeuroImage 45(2):319–332. https://doi.org/10.1016/j.neuroimage.2008.11.014
Paillard T, Noé F (2015) Techniques and methods for testing the postural function in healthy and pathological subjects. BioMed Res Int 2015 2015:891390. https://doi.org/10.1155/2015/891390
Pascual-Marqui RD, Michel CM, Lehmann D (1995) Segmentation of brain electrical activity into microstates: model Estimation and validation. IEEE Trans Biomed Eng 42(7):658–665. https://doi.org/10.1109/10.391164
Pascual-Marqui RD, Lehmann D, Faber P, Milz P, Kochi K, Yoshimura M, Kinoshita T (2014) The resting microstate networks (RMN): cortical distributions, dynamics, and frequency specific information flow. arXiv preprint arXiv:1411.1949.
Peterka RJ (2002) Sensorimotor integration in human postural control. J Neurophysiol 88(3):1097–1118. https://doi.org/10.1152/jn.2002.88.3.1097
Peterson P SM, Ferris DP (2018) Differentiation in Theta and Beta electrocortical activity between visual and physical perturbations to walking and standing balance. eNeuro 5(4):ENEURO0207–182018. https://doi.org/10.1523/ENEURO.0207-18.2018
Pion-Tonachini L, Kreutz-Delgado K, Makeig S (2019) ICLabel: an automated electroencephalographic independent component classifier, dataset, and website. NeuroImage 198:181–197. https://doi.org/10.1016/j.neuroimage.2019.05.026
Pollock AS, Durward BR, Rowe PJ, Paul JP (2000) What is balance? Clin Rehabil 14(4):402–406. https://doi.org/10.1191/0269215500cr342oa
Reason JT, Brand JJ (1975) Motion sickness. Academic, London
Recenti M, Ricciardi C, Aubonnet R, Picone I, Jacob D, Svansson HÁR, Agnarsdóttir S, Karlsson GH, Baeringsdóttir V, Petersen H, Gargiulo P (2021) Toward predicting motion sickness using virtual reality and a moving platform assessing brain, muscles, and heart signals. Front Bioeng Biotechnol 9:635661. https://doi.org/10.3389/fbioe.2021.635661
Recenti M, Jacob D, Aubonnet R et al (2022) Predicting lifestyle using BioVRSea multi-biometric paradigms. In: Proc 2022 IEEE Int Conf Metrol Ext Reality Artif Intell Neural Eng pp 329–334. https://doi.org/10.1109/MetroXRAINE54828.2022.9967685
Richer N, Bradford JC, Ferris DP (2024) Mobile neuroimaging: what we have learned about the neural control of human walking, with an emphasis on EEG-based research. Neurosci Biobehav Rev 162:105718. https://doi.org/10.1016/j.neubiorev.2024.105718
Roberts RE, Ahmad H, Arshad Q, Patel M, Dima D, Leech R, Seemungal BM, Sharp DJ, Bronstein AM (2017) Functional neuroimaging of visuo-vestibular interaction. Brain Struct Funct 222(5):2329–2343. https://doi.org/10.1007/s00429-016-1344-4
Si X, Huang H, Yu J, Ming D (2024) EEG microstates and fNIRS metrics reveal the Spatiotemporal joint neural processing features of human emotions. IEEE Trans Aff Comp 15(4):2128–2138. https://doi.org/10.1109/TAFFC.2024.3399729
Sibley KM, Mochizuki G, Lakhani B et al (2014) Autonomic contributions in postural control: a review of the evidence. Rev Neurosci 25(5):687–697. https://doi.org/10.1515/revneuro-2014-0011
Solis-Escalante T, van der Cruijsen J, de Kam D et al (2019) Cortical dynamics during Preparation and execution of reactive balance responses with distinct postural demands. NeuroImage 188:557–571. https://doi.org/10.1016/j.neuroimage.2018.12.045
Stephan T, Deutschländer A, Nolte A, Schneider E, Wiesmann M, Brandt T, Dieterich M (2005) Functional MRI of galvanic vestibular stimulation with alternating currents at different frequencies. NeuroImage 26(3):721–732. https://doi.org/10.1016/j.neuroimage.2005.02.049
Takakusaki K (2017) Functional neuroanatomy for posture and gait control. J Mov Disord 10(1):1–17. https://doi.org/10.14802/jmd.16062
Takakusaki K (2023) Gait control by the frontal lobe. Handb Clin Neurol 195:103–126. https://doi.org/10.1016/B978-0-323-98818-6.00021-2
Tarailis P, Koenig T, Michel CM et al (2024) The functional aspects of resting EEG microstates: a systematic review. Brain Topogr 37:181–217. https://doi.org/10.1007/s10548-023-00958-9
Weech S, Kenny S, Barnett-Cowan M (2019) Presence and cybersickness in virtual reality are negatively related: a review. Front Psychol 10:158. https://doi.org/10.3389/fpsyg.2019.00158